04

The influence of the exposed electrode material on the development of surface barrier discharge in air

© I.V. Selivonin,[1] A.V. Lazukin,[2] I.A. Moralev[1]

[1] Joint Institute for High Temperatures, Russian Academy of Sciences,
125412 Moscow, Russia
[2] National Research University „Moscow Power Engineering Institute“,
111250 Moscow, Russia
e-mail: inock691@ya.ru

Received March 12, 2025
Revised April 18, 2025
Accepted May 19, 2025

The aim of this work is to study the influence of the exposed electrode material on the dynamics of the surface dielectric barrier discharge characteristics during its long-term operation. A comparison of the structure and dynamics of the discharge power during continuous operation for 200 min on electrodes made of copper, nickel, molybdenum and aluminum was carried out. The discharge on copper and nickel electrodes has a high degree of non-uniformity along the electrode span. In the case of aluminum and molybdenum electrodes, the discharge looks like a diffuse glow region. During long-term operation of the discharge on copper and molybdenum electrodes, a noticeable increase in the power dissipated in the discharge is observed, while in the case of nickel and aluminum electrodes, it decreases. The reason for the different behavior of the electrodes during modification in the discharge is the binding energy of the oxides and their electrical conductivity.

Keywords: gas discharge, barrier discharge, electrode modification, electrode durability.

DOI: 10.61011/TP.2025.11.62232.33-25

Introduction

Surface barrier discharge (SBD) is a high-pressure discharge initiated in a system of two or more electrodes separated by a dielectric barrier [1–3]. This type of discharge can be used to solve numerous technological problems in the field of plasmochemistry [4,5], processing of biological objects [6,7], plasma aerodynamics [8,9], plasma surface treatment of metals [10,11] and polymers [12–14].

The discharge is usually powered by alternating or pulsed voltage. When the potential of the corona electrode changes relative to the barrier surface, threshold values of the electric field strength at the edge of the electrode are reached, which leads to a discharge. During the development of the discharge, charge is transferred to the surface of the barrier and accumulates in the volume near the edge of the corona electrode. The intrinsic electric field of this charge shields the field of the electrode, as a result of which the development of the discharge stops [15]. Since the relaxation time of the charge on the surface of most dielectrics is quite long, the discharge can occur again only with a further increase in the potential of the electrode. If the potential on an open electrode changes monotonously, then each time a certain field strength is reached, the process of discharge development repeats. In air, under normal conditions, a barrier discharge exists in the form of separate microdischarges, each of which corresponds to a current pulse with a duration of about 10−100 ns and an amplitude of less than 1 A [16,17].

In most cases, the resource of discharge systems based on SBD is associated with the degradation of the dielectric barrier [18–21]. The initiation of a discharge on dielectrics made of polymers and other organic materials leads to intense local melting and evaporation of the material, which ultimately leads to the breakdown of the barrier and the transition of a low-current discharge into a spark form. The life of the system is determined by the degradation of the electrodes in case of usage of dielectric barriers made of discharge-resistant materials [22–24].

The change in the structure of the corona edges during discharge combustion in air was studied in Ref. [25,26]. It was demonstrated in Ref. [27] that the change in the edge structure during discharge operation in an oxygen-containing medium is determined by the balance of competing processes of erosive purification of the electrode from oxides (as a result of ion bombardment in the cathode spots of microdischarges) and the formation of an altered surface layer on the electrode (as a result of thermal oxidation, implantation and diffusion of oxygen ions deep into the electrode, as well as recycling of the eroded material). At the same time, significant changes can also be observed in the case of the production of electrodes from precious metals [23,24]. Modification of the electrodes can have a significant impact on various characteristics of the discharge, for example, the power dissipated in the discharge [23,25] and its structure [25,28], characteristics and statistics of individual microdischarges [17]. The formation of an oxide layer on the corona edge can lead to a change in the shape

of the pulse current at the initial stage of the development of the microdischarge [29]. This indicates significant changes in the emission properties of the electrode associated with the accumulation of charge on the surface of the oxide film [30], a change in the operation of the electron output [31] and an electrical breakdown of the oxide layer at the start of the microdischarge [32].

The purpose of this paper is to study the degradation processes of electrodes in barrier discharges and devices based on them: ozonators, plasma chemical reactors, biological sample processing systems. The structure and electrical characteristics of a discharge in air on electrodes made of metals, the oxides of which have significantly different properties, such as the resistance of the oxide to cathode sputtering and electrical conductivity, have been studied for this purpose.

1. Experimental setup and methods

A barrier discharge in a surface asymmetric configuration „edge-plane“ was studied in this paper. A schematic diagram of a discharge cell with a connection diagram is shown in Fig. 1.

The discharge cell consisted of open (corona) and counter (grounded) electrodes and a dielectric barrier made of VK-94 alumina ceramics with a thickness of 1 mm and a dielectric constant of about 10 separating them. The edge span of the electrodes was 30 mm. The counter electrode was coated with a silicone compound to prevent the development of a discharge on the reverse side of the barrier. To prevent significant heating, the cell was placed on the radiator. The maximum temperature of the electrode system during the experiment did not exceed 60 °C.

All studies were conducted in synthetic air at atmospheric pressure and room temperature. To control the composition

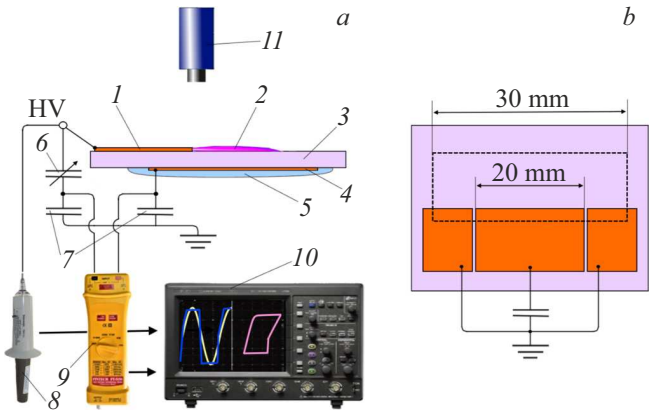

Figure 1. *a* — image of a discharge cell with a connection diagram: *1* — open (corona) electrode, *2* — surface barrier discharge, *3* — ceramic barrier, *4* — counter electrode, *5* — compound, *6* — adjusting capacitance C_{comp}, *7* — measuring capacitances C_m, *8* — high voltage probe, *9* — differential probe, *10* — oscilloscope, *11* — CCD camera; *b* — image of the response an electrode with a connection diagram.

Table 1. Standard enthalpy of formation of oxides of selected materials [33]

Oxide	$-\Delta H^0_{298.15}$, kJ/mol
CuO	162.1
Cu_2O	173.3
NiO	239.9
Ni_2O_3	485.7
MoO_2	589.9
MoO_3	745.7
Al_2O_3	1676.8

of the working medium, the discharge system was installed in a sealed chamber, where, after preliminary pumping, a weak flow of synthetic air (mixtures of 20,% O_2 and 79,% N_2) was supplied from the cylinder. The proportion of impurities, according to the specification of the mixture, did not exceed 1 % (mainly argon), the moisture content did not exceed 0.0005 % vol. The gas flow is necessary to prevent the accumulation of large concentrations of ozone synthesized during discharge operation.

The corona electrodes were made of foil with a thickness of 20 μm. Copper, nickel, molybdenum and aluminum are used as the electrode material. This choice of materials is attributable to significantly different values of the binding energy of the oxides of these metals (Table 1), which presumably should be the determining factor of electrode degradation. The electrodes were glued to the barrier using ethanol-based LaDoratura gilding glue with a controlled adhesive sublayer thickness of 2–3 μm. This made it possible to achieve maximum repeatability of the electrode geometry in the manufacture of various discharge cells. Before starting the experiment, the quality of the electrode edges was monitored for the absence of deformations and contamination, for which an optical stereo microscope MBS-10 was used.

The discharge was powered by an alternating sinusoidal voltage with an amplitude of 3.4 kV and a frequency of 110 kHz. With such voltage parameters, the values of the energy input density in the discharge are near-threshold for the onset of contraction. Presumably, in this mode, the fastest degradation rates for the streamer mode of discharge combustion are achieved on the studied discharge cell. The high voltage was generated by a transistor power supply connected to a resonant circuit. To adjust the voltage during the experiment, the excitation frequency of the circuit could vary within 5 % near the resonance.

During the experiment, the discharge operated continuously for 200 min. This duration of discharge exposure is due to the fact that with the supply voltage parameters used in operation (~ 100 kHz; 3.4 kV), the main significant changes associated with degradation of the electrode mate-

rial are expected during the first 60–120 min of discharge operation [25].

The oscillograms of the supply voltage and the charge transferred from the electrode to the surface of the dielectric were recorded during discharge combustion at intervals of 3–30 min. The transferred charge was measured from the central part of a 20 mm wide counter electrode connected to the ground via a measuring capacity $C_m = 2.2$ nF (ceramic capacitor KVI-3). The use of only the central section of the discharge in the analysis of its electrical characteristics made it possible to exclude from consideration its inhomogeneities at the edges and corners of the electrode. The side parts of the counter electrode, which were not involved in charge measurements, were connected directly to „ground". The measuring capacity is significantly larger than the discharge capacity $C_m \gg C_{dis} \sim 1 - 10$ pF [34], and the gap width in the underlying electrode is significantly less than the barrier thickness (and the characteristic scale of spatial organization of microdischarges under similar conditions [17]), so the measuring circuit has no effect on the development of discharge.

To exclude the capacitive current through the electrode system from measurements, a capacitor bridge was used, in the upper arm of which a tuning vacuum capacitor $C_{comp} = 3–50$ pF was installed. The Ccomp value was selected at voltages lower than the discharge initiation voltage (about 0.6–0.8 kV) so that the voltage difference across the measuring capacitances was zero. This measurement method is a modification of the method for recording the electrical characteristics of an HF discharge, presented in the literature [35]. The voltage difference across the measuring capacitances C_m was measured using a PintekDP-150 Pro differential probe (error 5 %, bandwidth 150 MHz). The high voltage was measured with a Tektronix P6015A high-voltage probe (accuracy 5 %, bandwidth 75 MHz). The data were collected using a LeCroy HDO6104AR oscilloscope with a bandwidth of 1 GHz and a vertical resolution of 12 bit. The data were averaged over 128 periods of supply voltage.

The power dissipated in the discharge was calculated using the volt-coulomb cyclograms (VCC) method [34,36–38]. The energy dissipated in the discharge during one voltage period can be determined by estimating the VCC area:

$$E_T = \int_{-U_a}^{+U_a} Q(t)dU(t) = C_m \int_{-U_a}^{+U_a} U_c(t)dU(t),$$

$$P = \frac{1}{T} E_T = f E_T,$$

where $U(t)$ and $U_c(t)$ are measured waveforms of the supply voltage and the voltage difference across the measuring capacitances C_m, f is the frequency of the supply voltage. A detailed justification of the applicability of power measurement by the VCC method for the configuration under study is given in Ref. [39]. The error of the received power dissipation values was about 10 %.

In addition to the electrical characteristics of the discharge, photographs of the discharge and the electrode edge were obtained. Micrographs were obtained using a CCD camera using an MBS-10 optical microscope with a 16x magnification. The discharge images were taken in the visible spectral range with an exposure of 30 ms.

Results

Changes in the brightness distribution of the discharge along the edge occur during the discharge combustion, which are accompanied by changes in its electrical characteristics.

Fig. 2 shows the dynamics of the discharge power at various electrodes. At the initial moment, the power dissipation values are almost the same and are at the level of 70 mW with 1 mm of edge. Further, in the case of copper and molybdenum electrodes, there is a slight increase in power over a time of about 60 min. In the case of aluminum and nickel electrodes, the power dissipated in the discharge drops significantly to the level of 20 mW/mm. In this case, the changes on the aluminum electrode occur much faster than on the nickel electrode.

Photos of the discharge on various electrodes are shown in Fig. 3. Initially, the discharge on all electrodes is not uniform along the edge. The brighter areas alternate with dark areas with a spatial period approximately corresponding to the length of the discharge.

When the discharge is continuously burned for more than 60 min, the discharge on the copper and nickel electrodes stabilizes and looks like a set of separate discharge flares distributed along the electrode. At the same time, the structure of the discharge on the copper electrode does not change noticeably until the end of the experiment, and in the

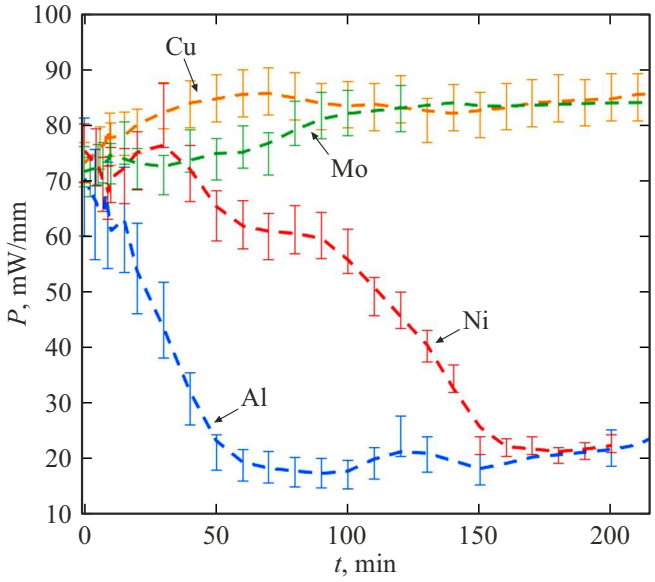

Figure 2. Dynamics of discharge power on electrodes made of various materials.

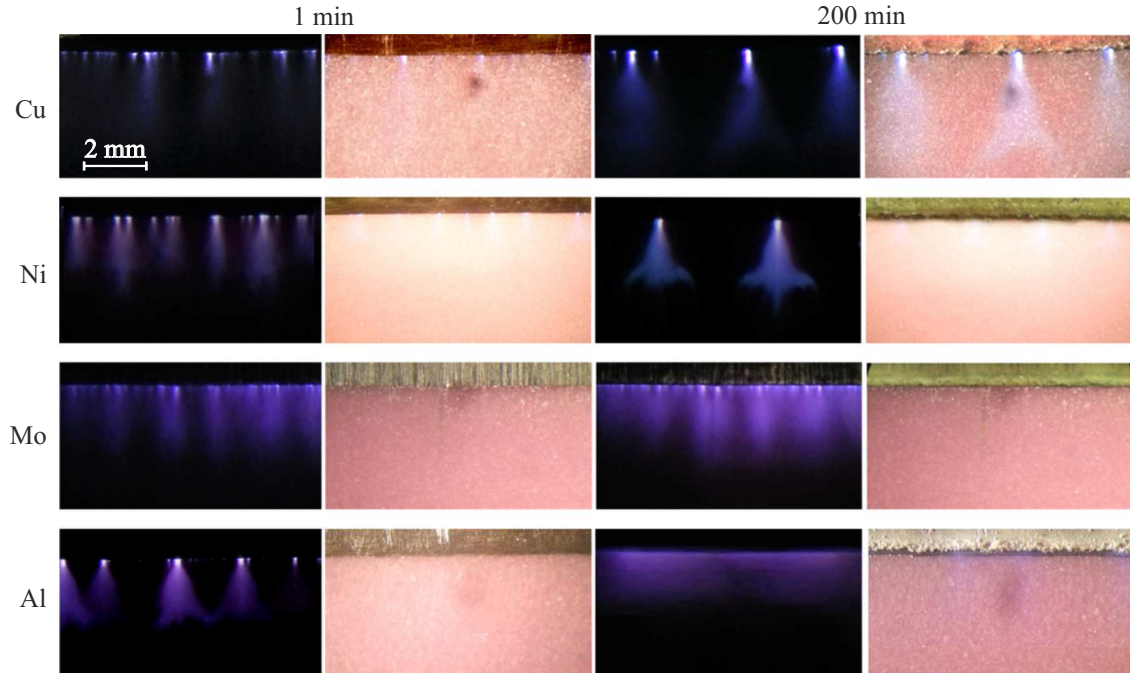

Figure 3. Images of discharge and electrodes made of various materials in the first minute of discharge operation and after continuous operation for 200 min. The frame exposure is 30 ms.

case of a nickel electrode, a gradual extinction of individual filaments is observed with a decrease in the „active“ area of the electrode from which the discharge develops.

The morphology of the edge on these electrodes undergoes significant changes. In the vicinity of the discharge flare attachment points, the formation of submillimeter-sized craters surrounded by products of the redeposition of oxides can be observed.

The discharge looks like a region of diffuse glow on the modified aluminum electrode. At the same time, the formation of a dark layer uniform in the span of the electrode can be observed on the corona edge. An analysis of the composition and structure of this layer, carried out earlier in the work of jcite25, showed that it is formed as a result of metal substitution at the electrode edge with Al_2O_3 oxide.

On a molybdenum electrode, the discharge practically does not change even after its operation for 200 min. Coupled with very small changes in power dissipation, this suggests that the properties of the molybdenum electrode change little during its modification in a barrier discharge.

The formation of oxide formations at the edge of the electrode affects the dynamics of microdischarges, as evidenced by distortions in the shape of the VCC discharge (Fig. 4). The development of each microdischarge corresponds to a VCC steps [16]. When VCC averaging a large number of stochastically developing microdischarges, the curves are smoothed. However, when synchronizing the start of multiple microdischarges along the edge, the step-like structure of the VCC is preserved. Fig. 4 shows that such synchronization is indeed observed in the positive half-cycle of the supply voltage (when the corona electrode is an anode) in the case of a filamentary discharge combustion, which is realized on electrodes made of copper and nickel. On the contrary, the discharge VCC on molybdenum and aluminum electrodes are smooth, which is explained by the random moment when surface streamers start from the edge of the electrode.

2. Discussion of the results

The most noticeable result of the electrode modification is a change in the uniformity of the discharge along the edge. Taking this effect into account can be extremely important when using a discharge to solve a number of applied problems. For example, this effect is important for plasma treatment of surfaces or biological objects [40,41], where the requirements of uniformity of processing and maximum energy storage density are imposed, or when controlling the flow using SBD-based actuators, where discharge inhomogeneities can lead to the induction of flows with a three-dimensional structure [42].

The physical mechanism responsible for changes in the observed discharge structure is a change in the dynamics of single microdischarges caused by edge modification. A detailed description of the organization of a filamentary mode with channel stabilization on a copper electrode and a quasi-diffusion mode on an aluminum electrode is given in Ref. [17,25]. On time scales of the order of the duration of the existence of one generation of microdischarges (less

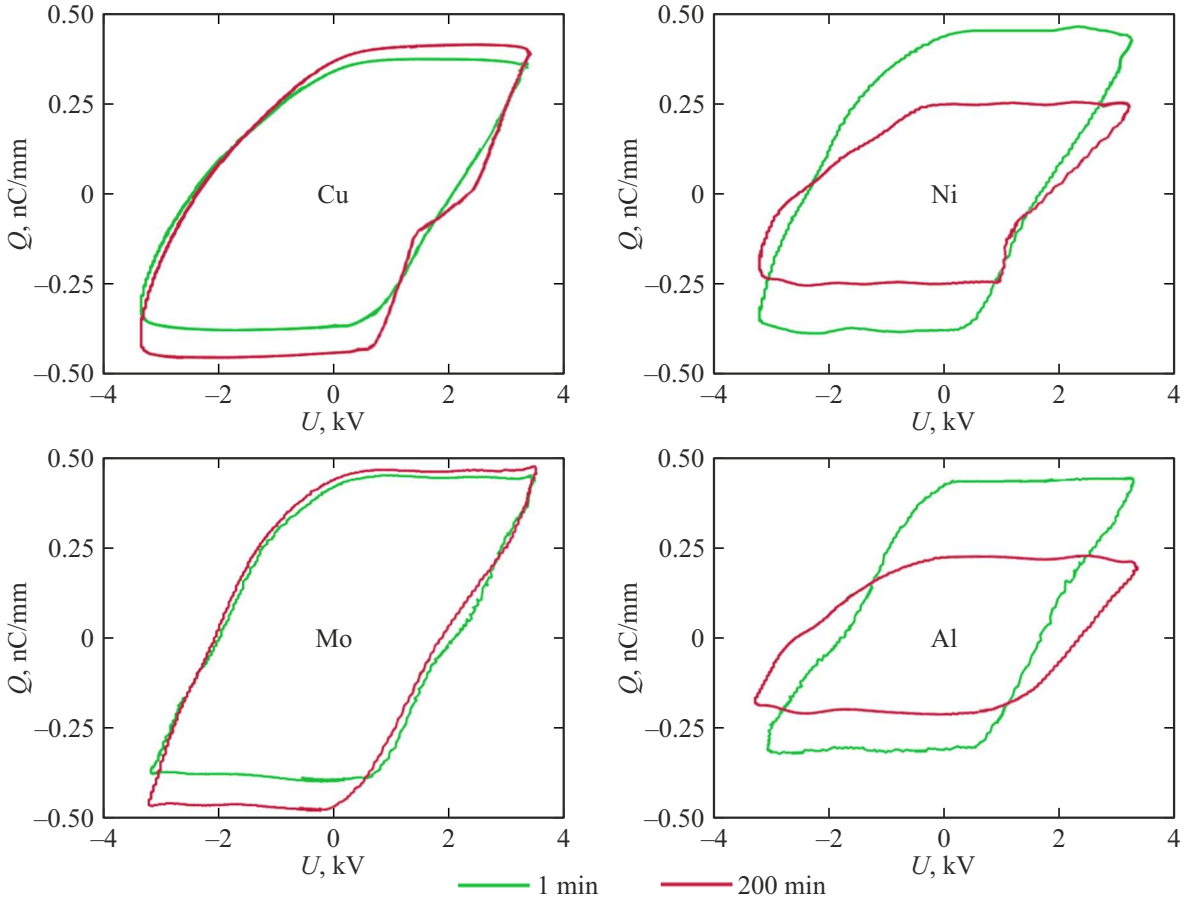

Figure 4. Averaged over 128 periods of the supply voltage of the VCC discharge on electrodes made of various materials at the time of ignition of the discharge and after continuous operation of the discharge for 200 min.

than 1 μs), the discharge looks like a set of channels distributed evenly along the edge span [17]. At the same time, the instantaneous structure of the discharge does not differ on electrodes made of different materials.

In the case of copper and nickel electrodes, the formation of local structures in the form of craters with an oxide rim leads to a strong heterogeneity of the electric field strength along the edge and localization of microdischarge bindings in the strong field region. As a result, microdischarges always start from the same sections of the electrode, and when averaged over long periods, the discharge looks like a set of isolated filaments. Tension inhomogeneities occur due to charging of the oxide rim during discharge combustion, as well as local edge deformation in the crater region, which can significantly change the threshold voltage of the start of microdischarges in this region [43].

The aluminum electrode along the edge is covered with a micron-thick porous oxide layer. With the development of a microdischarge, local charging of the formed dielectric layer occurs, which leads to the shielding of the field in this area. As a result, the next microdischarges start from other areas of the electrode, and for long observation times, the discharge is almost uniform along the edge.

The molybdenum electrode is also coated with a homogeneous layer, presumably consisting of an oxide, but the modification of the edge does not lead to noticeable changes in the characteristics of the discharge.

It was shown in Ref. [27] that the electrode material has practically no effect on the structure of the discharge in the absence of oxygen. The main a priori hypotheses about the causes of the different processes of modification of electrodes made of different materials in an oxygen-containing environment are the resistance of the material itself and its oxide to cathode sputtering. Table 2 shows some properties of oxides, which presumably can influence the modification of the edge. The parameters of tungsten oxides are given for comparison in addition to the materials used in the study. It was demonstrated in Ref. [28] that after prolonged combustion on a tungsten electrode, the discharge is much more uniform than on a copper one.

It can be seen that among the materials used, there is a clear correlation between the degree of uniformity of the discharge and the power dynamics during electrode training with the value of the enthalpy of oxide formation.

During ion bombardment of the electrode surface, the ion penetrates to a certain depth and initiates a cascade of

Table 2. Properties of various metal oxides of open electrodes

Oxide	$-\Delta H^0_{298.15}$, kJ/mol	Melting point, °C	Evaporation temperature, °C	R, Ω·m
CuO	162.1	1336	2000(decomposing)	Semiconductor $10^0 - 10^1$ (20 °C) $5 \cdot 10^{-2}$ (700 °C)
Cu_2O	173.3	1242	1800 (decomposing)	Dielectric $10^6 - 10^7$ (20 °C) 70 (130 °C)
NiO	239.9	1957 (decomposing)	–	Dielectric 1011 (20 °C) 101 (590 °C)
MoO_2	589.5	1927	1977 (decomposing)	Explorer $2 \cdot 10^{-2}$ (20 °C) [48]
WO_2	589.9	1570	1852 (decomposing)	Semiconductor 10^1 (20 °C) [48]
MoO_3	745.7	795	1155	Dielectric 10^4 (20 °C) [49]
WO^3	843.2	1473 – 2130	1850 10^4 (20 °C) [50]	Dielectric
Al_2O_3	1676.8	2046.5	2980	Dielectric 10^{14} (10 °C) $3 \cdot 10^{10}$ (400 °C)

Note: The data for which the source is not specified are taken from [33].

atomic collisions in the electrode material, which can lead to the breaking of the bond of atoms on the electrode surface and their sputtering [44,45]. If in the case of inert ions their capture is possible only by structural defects of the surface layer of the target, then in the case of chemically active ions chemical reactions occur between them and the atoms of the target. In this case, a modified surface layer is formed [46,47]. With prolonged exposure to the beam, an equilibrium concentration of trapped ions is achieved, determined by the ratio of the rate of ion implantation and their removal due to sputtering, as well as the ratio of diffusion fluxes deep into the target and to its surface. Finally, the formation of a modified surface layer may be accompanied by its heating if the chemical reactions are exothermic. If the formed compound has a low binding energy, then its molecules and atoms can leave the target surface when it is heated as a result of desorption.

The properties of the modified surface layer differ from those of the target material, and its formation leads to a change in the sputtering characteristics. Sputtering of the oxide layer from the electrode can be considered as spraying of a multicomponent substance. The partial sputtering coefficients of each component vary. As a rule, the lightest component is sputtered most intensively in a multicomponent system. Thus, when sputtering oxide layers, in the case when the metal is heavier with respect to oxygen, the oxide is converted directly on the surface of the layer into a form with a lower degree of oxidation, if such exists, or the surface is metallized.

The density of the ion current on the electrode surface is approximately the same for all the materials considered in the work at the time of the first ignition of the discharge, since the values of the power dissipated in the discharge coincide at the initial moment, and the structure of the discharge is similar. The rates of ion implantation deep into the material and ohmic heating of the electrode presumably also differ slightly. However, the removal of oxygen from surface areas significantly depends on the binding energy of the atoms in the oxides, therefore, as it increases, the balance of the active mechanisms will shift from local erosion treatment to surface oxidation.

The organization of a filamentary discharge combustion leads to an increase in power dissipation. This is due to the local heating of the gas in the channel stabilization area. The discharge develops in a thermal cavity, which leads to an increase in its length and, accordingly, the charged surface area of the barrier. In addition, it was demonstrated in Ref. [17] that channel stabilization leads to an increase in the role of electron detaching mechanisms from negative oxygen ions, which leads to a significant increase in the duration of currents in microdischarges.

If the intensity of oxide spraying from the surface is insufficient, after the organization of a filamentary discharge combustion, a gradual fading of the channels can be observed. This leads to a decrease in power dissipation, which is observed in the case of a nickel electrode, and has also been demonstrated for a copper electrode with reduced supply voltage parameters (lower amplitude and frequency) [17,39].

The behavior of the molybdenum electrode does not fit into the framework of the described patterns. Its oxides have a high binding energy, so the electrode modification processes should be similar to those on an aluminum electrode. However, there are no noticeable changes in the discharge structure over time, and the power dissipated in the discharge increases. This can be explained by the abnormally high electrical conductivity of MoO_2 for the oxide [44]. When the molybdenum electrode is modified, the memory effect associated with charging the oxide layer does not occur. The discharge is affected only by a change in the geometry of the edge (height above the barrier surface and defects in the electrode edge). During the formation and redeposition of oxides, dendrite-like structures are formed at the edge of the electrode [25]. They work as field sharpeners, which leads to a decrease in the start voltage of microdischarges, and can lead to an explosive electron emission mechanism, which will increase the current of microdischarges [51]. On average, this leads to an increase in the transferred charge and energy input into the discharge.

It should be noted that the intensity of cathode sputtering is influenced by factors such as the energy of incident ions and the frequency of microdischarges. Therefore, changes in the pressure of the medium, as well as the amplitude and frequency of the supply voltage, can shift the balance of the processes in the direction of atomization or oxidation of the edge.

Conclusion

The effect of the material and the state of the corona edge of the electrode in the SBD on the structure of the discharge and the amount of power dissipated in the discharge is studied. The structure and dynamics of the discharge power during continuous operation for 200 min in air on electrodes made of copper, nickel, molybdenum and aluminum are compared.

During discharge combustion, the electrode is subjected to local ion bombardment in the cathode spots of the microdischarges. In this case, oxygen ions are implanted deep into the electrode material, as well as kinetic and chemical cathode sputtering of the surface layers. The first mechanism leads to the accumulation of oxygen in the surface layers, and its rate weakly depends on the properties of the electrode material and its oxides. The second mechanism, on the contrary, promotes the purification and metallization of the electrode at the binding sites of the microdischarges, and the sputtering rate strongly depends on the binding energy of the oxide.

Based on the results obtained, it is possible to formulate the main trends in the modification of electrodes in a barrier discharge and the associated dynamics of discharge characteristics. With a low binding energy of oxides (copper electrode), the mechanism of local erosion cleaning of the electrode in the cathode spots of the microdischarge dominates. This leads to the formation of a structure in the form of submillimeter-sized craters on the edge, in the center of which a cathode layer of subsequent microdischarges is formed on an area free of oxide. As a result, a stable, filamentary discharge combustion mode is organized with local gas heating at the channel stabilization sites, which is accompanied by a noticeable increase in power dissipated in the discharge. At high values of the binding energy of the oxide of the electrode material (nickel electrode), a structure in the form of craters is also formed, but the intensity of erosion cleaning is insufficient to remove the oxide from the electrode, as a result of which individual channels fade over time. In this case, after a slight increase in power dissipation corresponding to the primary change in the structure of the discharge, its decrease is observed when the channels fade and the effective area of the electrode decreases. At high values of the binding energy of the oxide (aluminum and molybdenum electrodes), there is no noticeable erosion cleaning of the oxide edge, therefore, an altered surface layer is created on the electrode as a result of ion implantation. If the layer material is non-conductive (aluminum oxide), then its surface charging contributes to the spatial and temporal stochastization of microdischarges and a noticeable decrease in the power dissipated in the SBD. If the surface layer has a high conductivity (molybdenum oxide), then there are no noticeable changes in the properties of the discharge.

The intensity of cathode sputtering, in addition to the properties of the oxide, is affected by the energy of ions arriving at the electrode and the intensity of local heating of the electrode, therefore, changes in the pressure of the medium, as well as the amplitude and frequency of the supply voltage, can shift the balance of processes towards atomization or oxidation of the edge compared with the results demonstrated in the paper. Therefore, the described patterns are a qualitative comparison of the discharge behavior for different electrode materials under similar other conditions.

Funding

The work was carried out with the support of the Russian Science Foundation as part of the scientific project No.24-79-00168.

Conflict of interest

The authors declare that they have no conflict of interest.

References

[1] U. Kogelschatz, B. Eliasson, W. Egli. J. PHYS IV Fr., **7**, 4 (1997). DOI: 10.1051/jp4:1997405

[2] R. Brandenburg. Plasma Sources Sci. Technol., **26** (5), 053001 (2017). DOI: 10.1088/1361-6595/aa6426

[3] V.I. Gibalov, G.J. Pietsch. J. Phys. D. Appl. Phys., **33** (20), 2618 (2000). DOI: 10.1088/0022-3727/33/20/315

[4] N. Bednar, J. Matović, G. Stojanović. J. Electrostat., **71**, 1068 (2013). DOI: 10.1016/j.elstat.2013.10.010

[5] J. Mikeš, S. Pekárek, I. Soukup. J. Appl. Phys., **120**, 173301 (2016). DOI: 10.1063/1.4966603

[6] Y. Park, S.K. Oh, J. Oh, D.C. Seok, S.B. Kim, S.J. Yoo, M.-J. Lee, C.Y. Park. Plasma Process Polym., **15** (2), 1 (2016). DOI: 10.1002/ppap.201600056

[7] A.V. Lazukin, Y.A. Serdyukov, I.A. Moralev, I.V. Selivonin, S.A. Krivov. J. Phys. Conf. Ser., **1147** (1), 012124 (2019). DOI: 10.1088/1742-6596/1147/1/012124

[8] E.J. Moreau. Phys. D. Appl. Phys., **40** (3), 605 (2007). DOI: 10.1088/0022-3727/40/3/S01

[9] T.C. Corke, E.J. Jumper, M.L. Post, D. Orlov, T.E. McLaughlin. 40th AIAA Aerosp. Sci. Meet. Exhib.(c), (2002). DOI: 10.2514/6.2002-350

[10] L. Bónová, A. Zahoranová, D. Kováčik, M. Zahoran, M. Mičušík, M. Černák. Appl. Surf. Sci., **331**, 79 (2015). DOI: 10.1016/j.apsusc.2015.01.030

[11] D. Minzari, P. Møller, P. Kingshott, L.H. Christensen, R. Ambat. Corros. Sci., **50** (5), 1321 (2008). DOI: 10.1016/j.corsci.2008.01.023

[12] G. Borcia, C.A. Anderson, N.M.D. Brown. Plasma Sources Sci. Technol., **12** (3), 335 (2003). DOI: 10.1088/0963-0252/12/3/306

[13] K.G. Donohoe, T.J. Wydeven. Appl. Polym. Sci., **23** (9), 2591 (1979). DOI: 10.1002/app.1979.070230905

[14] D.J. Upadhyay, N.Y. Cui, C.A. Anderson, N.M.D. Brown. Appl. Surf. Sci., **229**, 352 (2004). DOI: 10.1016/j.apsusc.2004.02.012

[15] R. Brandenburg. Plasma Sources Sci. Technol., **26** (5), 053001 (2017). DOI: 10.1088/1361-6595/aa6426

[16] T. Hoder, P. Synek, J. Vorac. Plasma Sources Sci. Technol., **28** (10), 105016 (2019). DOI: 10.1088/1361-6595/ab4b91

[17] I.V. Selivonin, I.A. Moralev. Plasma Sources Sci. Technol., **30** (3), 035005 (2021). DOI: 10.1088/1361-6595/abe0a1

[18] M. Šimor, J. Rá hel', P. Vojtek, M. Černák, A. Brablec. Appl. Phys. Lett., **81** (15), 2716 (2002). DOI: 10.1063/1.1513185

[19] J. Pons, L. Oukacine, E. Moreau, J.M. Tatibouët. IEEE Trans. Plasma Sci., **36** (4), 1342 (2008). DOI: 10.1109/TPS.2008.926856

[20] A.R.H. Rigit, K.C. La, D.B.L. Bong. Proc. IEEE Int. Conf. Prop. Appl. Dielectr. Mater., **569** (2009). DOI: 10.1109/ICPADM.2009.5252365

[21] R.E. Hanson, J. Kimelman, N.M. Houser, P. Lavoie. 51st AIAA Aerosp. Sci. Meet. Incl. New Horizons Forum Aerosp. Expo. 2013 (January), **1** (2013). DOI: 10.2514/6.2013-397

[22] W. Changquan, H. Xiangning. Appl. Surf. Sci., **253** (2), 926 (2006). DOI: 10.1016/J.APSUSC.2006.01.032

[23] E. Pescini, M.G. De Giorgi, L. Francioso, A. Taurino, M.C. Martucci, Ph. Lavoie. 54th AIAA Aerosp. Sci. Meet. (January), 1 (2016). DOI: 10.2514/6.2016-0196

[24] I. Selivonin, A. Lazukin, I. Moralev, S. Krivov, I.J. Roslyakov. Phys. Conf. Ser., **1394**, 012027 (2019). DOI: 10.1088/1742-6596/1394/1/012027

[25] I.V.Selivonin, A.V. Lazukin, I.A. Moralev, S.A. Krivov. Plasma Sources Sci. Technol., **27** (8), 085003 (2018). DOI: 10.1088/1361-6595/aacbf5

[26] A.V. Lazukin, I.V. Selivonin, I.A. Moralev, S.A. Krivov. J. Phys. Conf. Ser., **927**, 012028 (2017). DOI: 10.1088/1742-6596/927/1/012028

[27] I. Selivonin, I. Moralev. J. Phys. Conf. Ser., **2100**, 012014 (2021). DOI: 10.1088/1742-6596/2100/1/012014

[28] N.M. Houser, L. Gimeno, R.E. Hanson, T. Goldhawk, T. Simpson, P. Lavoie. Sensors Actuators A. Phys., **201**, 101 (2013). DOI: 10.1016/j.sna.2013.06.005

[29] I.V. Selivonin, S.E. Kuvardin, I.A. Moralev. Bestnik OIVT RAN, **11**, 4 (2023) (in Russian).

[30] X. Yao, N. Jiang, B. Peng, Y. Xia, N. Lu, K. Shang, J. Li, Y. Wu. Vacuum, **166**, 114 (2019). DOI: 10.1016/j.vacuum.2019.04.035

[31] M. Černák, T. Hosokawa, S. Kobayashi, T.J. Kaneda. Appl. Phys., **83** (11), 5678 (1998). DOI: 10.1063/1.367422

[32] P.P. Budenstein, P.J. Hayes. J. Appl. Phys., **38** (7), 2837 (1967). DOI: 10.1063/1.1710011

[33] G.V. Samsonov *Physiko-khimicheskie svoystva okislov* (Metallurgiya, M., 1978) (in Russian)

[34] J. Kriegseis, B. Möller, S. Grundmann, C. Tropea. J. Electrostat., **69** (4), 302 (2011). DOI: 10.1016/j.elstat.2011.04.007

[35] M.A. Aronov, V.P. Larionov (red.) *Elektricheskaya izolyaciya vysokochastotnyh ustanovok vysokogo napryazheniya* (AO „Znak", M., 1994) (in Russian).

[36] J. Kriegseis, S. Grundmann, C. Tropea. J. Appl. Phys., **110**, 013305 (2011). DOI: 10.1063/1.3603030

[37] N.Y. Lysov. Elektrichestvo, **10**, 28 (2016) (in Russian).

[38] M.M. Pashin, N.Y. Lysov. Elektrichestvo, **12**, 21 (2011) (in Russian).

[39] I.V. Selivonin. *Vliyanie degradacii koroniruyushchego elektroda na harakteristiki poverhnostnogo bar'ernogo razryada* (Kand. diss. 1.3.9., M., 2022), p. 162 (in Russian).

[40] F. Massines, G. Gouda. J. Phys. D. Appl. Phys., **31** (24), 3411 (1998). DOI: 10.1088/0022-3727/31/24/003

[41] H.E. Wagner, R. Brandenburg, K.V. Kozlov, A. Sonnenfeld, P. Michel, J.F. Behnke. Vacuum, **71** (3 SPEC.), 417 (2003). DOI: 10.1016/S0042-207X(02)00765-0

[42] I. Moralev, V. Bityurin, A. Firsov, V. Sherbakova, I. Selivonin, M. Ustinov. Proc IMechE Part G J. Aerosp. Eng., **234** (1), 42 (2020). DOI: 10.1177/0954410018796988

[43] V.R. Soloviev, I.V. Selivonin, I.A. Moralev. Phys. Plasmas, **24**, 103528 (2017). DOI: 10.1063/1.5001136

[44] R. Berish. *Raspylenie tverdyh tel ionnoj bombardirovkoj* (Mir, M., 1984), v. I. (in Russian).

[45] N.V. Pleshivcev. *Katodnoe raspylenie* (Atomizdat, M., 1968) (in Russian).

[46] R. Berish. *Raspylenie tverdyh tel ionnoj bombardirovkoj* (Mir, M., 1986), v. II. (in Russian).

[47] S. Izman, M.R. Abdul-Kadir, M. Anwar, E.M. Nazim, R. Rosliza, A. Shah, M.A. Hassan. *Titanium Alloys — Towards Achieving Enhanced Properties for Diversified Applications* (IntechOpen, 2012), DOI: 10.5772/1928

[48] L. Ben-Dor, Y. Shimoni. Mater. Res. Bull., **9** (6), 499 (1974). DOI: 10.1016/0025-5408(74)90120-2

[49] R.B. Bennie, C. Joel, A.N.P. Raj, A.J. Antony, S.I. Pillai. J. Solid State Electrochem., **27** (1), 271 (2023). DOI: 10.1007/s10008-022-05319-3
[50] S.A. Kozyukhin, S.A. Bedin, P.G. Rudakovskaya, O.S. Ivanova, V.K. Ivanov. FTP, **52** (7), 745 (2018) (in Russian). DOI: 10.21883/ftp.2018.07.46046.8719
[51] G.A. Mesyats. UFN, **165** (6), 601 (1995) (in Russian).

Translated by A.Akhtyamov